[4] Singleton, R. E., Nash, J. F., Carr, L. W., and Patel, V. C., "Unsteady Turbulent Boundary-Layer Analysis," TM X-62, 242, Feb. 1973, NASA.

[5] Singleton, R. E. and Nash, J. F., "A Method for Calculating Unsteady Turbulent Boundary Layers in Two- and Three-Dimensional Flows," *Proceedings of the AIAA Computational Fluid Dynamics Conference*, July 1973, AIAA, Palm Springs, Calif.

[6] Nash, J. F. and Patel, V. C., "A Generalized Method for the Calculation of Three-Dimensional Turbulent Boundary Layers," *Fluid Dynamics of Unsteady, Three-Dimensional and Separated Flows*, Proceedings of Project SQUID Workshop, Georgia Institute of Technology, Atlanta, Ga., June 1971.

[7] Nash, J. F. and Patel, V. C., *Three-Dimensional Turbulent Boundary Layers, SBC Technical Books*, Sybucon, Inc., Atlanta, Ga., 1972.

[8] Bradshaw, P., Ferriss, D. H., and Atwell, N. P., "Calculations of Boundary-Layer Development Using the Turbulent Energy Equation," *Journal of Fluid Mechanics*, Vol. 28, 1967, p. 593.

[9] Bradshaw, P., "Calculation of Boundary Layer Development Using the Turbulent Energy Equation, VI, Unsteady Flow," NPL Aerospace Rept. 1288, Feb. 1969, National Physical Laboratory, England.

[10] Sears, W. R. and Telionis, D. P., "Unsteady Boundary-Layer Separation," *Recent Research on Unsteady Boundary Layers (Proceedings of the IUTAM Symposium*, Quebec 1971), edited by E. A. Eichelbrenner, Presses de l'Université Laval, Quebec 1972.

FEBRUARY 1975 AIAA JOURNAL VOL. 13, NO. 2

Penetration of a Lateral Sonic Gas Jet into a Hypersonic Stream

WILLIAM G. REINECKE*
Avco Systems Division, Wilmington, Mass.

Experiments were conducted to measure the extent of the disturbance caused by large lateral sonic gas injection from a slender cone into a Mach 13 airstream. The variables in the tests were injectant gas, injectant mass flow, nozzle geometry, and freestream pressure altitude (or jet pressure ratio). The measured dependent variables were the jet penetration height and the height of the resultant shock wave in the freestream. Within the variable ranges tested the data showed that the jet behaved as a point source and that the nozzle cross-section shape was unimportant. The measured jet penetration heights were compared with the predictions from four formulae available in the literature. The formula of Zukoski and Spaid predicted the jet penetration height very well. In addition, it was shown that the local height of the shock in the freestream resulting from the injection could be predicted reasonably well, and in a manner consistent with the Zukoski and Spaid model, by considering the shock to be the result of a sphere placed in the freestream at the jet location having a radius equal to the jet penetration height.

Nomenclature

D_j = jet throat diameter
h = penetration height, jet shock height
k = the coefficient $h/r(\bar{m})^{1/2}$
m = injectant mass flow rate
$\bar{m}$ = $m/\rho_\infty u_\infty \pi r^2$
p_j^o = injectant gas total pressure
R = universal gas constant
r = cone base radius
s = interaction shock height
T_j^o = injectant gas total temperature
T_∞^o = freestream total temperature
u_∞ = freestream speed
$\mathcal{M}_j$ = injectant gas molecular weight
$\mathcal{M}_\infty$ = freestream molecular weight
γ_j = injectant gas specific heat ratio
ρ_∞ = freestream density

THE purpose of the tests and correlation described herein was to determine the size disturbance that can be produced by the discrete injection of a gas laterally into a hypersonic stream. Specifically, we wished to measure the height above the cone surface of the shock wave caused by large lateral gaseous injection and the variation of this height with jet characteristics and to assess the accuracy of various analytical models in predicting the shock height. The independent variables in the tests were the mass flow, injectant gas, injector nozzle geometry, and pressure altitude. The test geometry, Mach number, and injectant stagnation temperature (about 70°F) and pressure (about 50 psia) were fixed. The model was a 6° half angle cone, 0.5 in. in base radius with variable geometry sonic injection nozzles located 180° apart and 0.20 in. forward of the cone base plane. The axes of the jets were normal to the cone centerline. The sizes of the interactions on the opposite sides of the cone were independent at even the highest injection rates. This was observed in preliminary tests in which gas was injected at a constant rate on one side of the cone while the injection rate on the other side was varied from zero to maximum.

The test conditions are given in Table 1. The tests were conducted in Avco's 20 in. diam shock tunnel and most of the data were obtained at Mach 13.2 and at 151,000 ft pressure altitude. The corresponding freestream Reynolds number based on cone base radius was 52,700. At this condition three injector nozzle cross-sectional geometries were used (circles, and 5 and 10 to 1 rectangles with their longer sides normal to the exterior flow direction), and four different gases were injected (N_2, Xe, He, and Freon 116) at various mass flow rates. The injectant mass flow rate was controlled by the jet throat area. The tests at 168,000 and 195,000 ft pressure altitude were conducted with nitrogen flowing from slot nozzles only and were directed at determining the effect, if any, of injectant stagnation to freestream pressure ratio (or altitude) independent of the other test variables.

Received February 13, 1974; revision received August 23, 1974. This work was supported by the U.S. Air Force Systems Command, Space and Missile Systems Organization under Contract F04-701-71-C-0002.

Index categories: Jets, Wakes, and Viscid-Inviscid Flow Interactions; Supersonic and Hypersonic Flow.

* Senior Consulting Scientist. Associate Fellow AIAA.

Table 1 Test conditions

Freestream Mach number	Freestream total temperature (°R)	Freestream total pressure (psia)	Freestream Reynolds number based on cone base radius	Pressure altitude (kft)	Freestream mass flux based on cone base area (millislugs/sec)	Ratio of jet stagnation to freestream pressure
13.2	3200	6300	52,700	151	0.555	1730–3730
12.9	3200	2820	25,200	168	0.277	8840–9280
12.4	3200	760	7,600	195	0.089	16,400–27,800

Some uncontrollable variation from test to test occurred in the jet stagnation pressure resulting in the ranges of jet stagnation to freestream pressure ratio shown in Table 1. Nevertheless, the uncontrolled spread in pressure ratio at each test condition was small with respect to the planned variation over the three test conditions and the purpose of isolating pressure ratio or altitude effects from variable mass flow and other effects was achieved.

Figures 1 and 2 are representative schlieren photographs of the disturbances caused by small and large blowing rates. As indicated in Fig. 1 the penetration height h was defined as the distance, in the plane of the cone base, from the cone surface to the strong shock embedded in the jet. This distance was shown clearly by the abrupt film density change in the schlieren photographs. The penetration height was measured in the plane of the cone base because the jet shock had its maximum height at approximately that location. Similarly the interaction shock height s was defined as the distance, also in the plane of the cone base, from the cone surface to the interaction shock wave. Two general aspects of the flow induced by the injection are apparent in these figures. Even at the lower flow rate the separation zone extends halfway to the cone tip, and at a dimensionless flow rate $\bar{m}$ of about three, the separation extends all the way to the cone tip. In this case the penetration or jet shock height is about 2.5 base radii and the interaction shock height is about four radii. The waviness of the interaction shock indicates that the interaction is unsteady. As will be seen later, this unsteadiness results in a variation in the measured instantaneous penetration height and interaction shock height.

Lateral jet penetration height correlations are generally presented as the ratio of penetration height to jet throat diam h/D_j. However, since our ultimate goal was to minimize the jet mass flow required to obtain a given external flow perturbation, it was more relevant and convenient in correlating the present data to use the ratio of penetration to cone base radius h/r considered as a function of dimensionless mass flow $\bar{m}$. The latter correlation is obtained from the former by the identity

$$\frac{h}{r} = 4\frac{h}{D_j}\bar{m}\frac{\rho_\infty u_\infty r}{p_j^o D_j}\left[\frac{RT_j^o}{\gamma_j \mathscr{M}_j}\left(\frac{\gamma_j+1}{2}\right)^{\gamma_j+1/\gamma_j-1}\right]^{1/2} \tag{1}$$

This form of the correlation explicitly introduces the injectant molecular weight and stagnation temperature as parameters and eliminates the injectant to freestream stagnation pressure ratio. Since the flow perturbations caused by the injection were larger than the cone shock layer thickness, the penetration data were correlated with the freestream conditions. Correlating the data in this manner ignores the details of the separation upstream of the injection but is consistent in that regard with the analytical models which we are trying to validate. Four formulae exist for predicting the penetration height h without employing foreknowledge of the separation region.[1-4] The first formula can be derived using blast wave theory and equating the force on the jet with the drag of the equivalent hypersonic spherical body (see, for example, Broadwell).[1] Suitably nondimensionalized, this yields

$$h/r = 2\left[\bar{m}\left(1 + \frac{\mathscr{M}_\infty}{\mathscr{M}_j}\frac{T_j^o}{T_\infty^o}\right)\right]^{1/2} \tag{2}$$

Similarly nondimensionalized, the work of Zukoski and Spaid,[2] Cassel, Davis, and Engh,[3] and Schetz[4] yield, respectively

$$\frac{h}{r} = 2\left(\frac{\gamma_j \bar{m}}{u_\infty}\right)^{1/2}\left[\frac{2RT_j^o}{\mathscr{M}_j\gamma_j(\gamma_j-1)}\right]^{1/4} \tag{3}$$

$$\frac{h}{r} = \frac{3}{2}\left(\frac{2\bar{m}}{u_\infty}\right)^{1/2}\left[\frac{2RT_j^o(\gamma_j+1)}{\mathscr{M}_j\gamma_j}\right]^{1/4} \tag{4}$$

and

$$\frac{h}{r} = \left(\frac{6\bar{m}}{u_\infty}\right)^{1/2}\left[\frac{2RT_j^o}{\mathscr{M}_j\gamma_j(\gamma_j+1)}\right]^{1/4} \tag{5}$$

The last correlation, Eq. (5), applies only when the injectant gas has a specific heat ratio of 1.4. Implicit in all these formulations are the assumptions that the jet acts as a point, not line, source and that all the gases are perfect. Although there is a similarity among these equations, they predict both qualitatively and quantitatively different effects of injectant gas properties on penetration height.

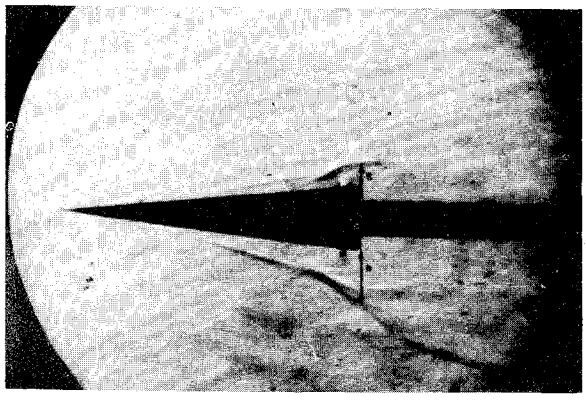

Fig. 1 Nitrogen injection, $\bar{m} = 0.70$, $M = 13.2$, $p_j^o = 70$ psia.

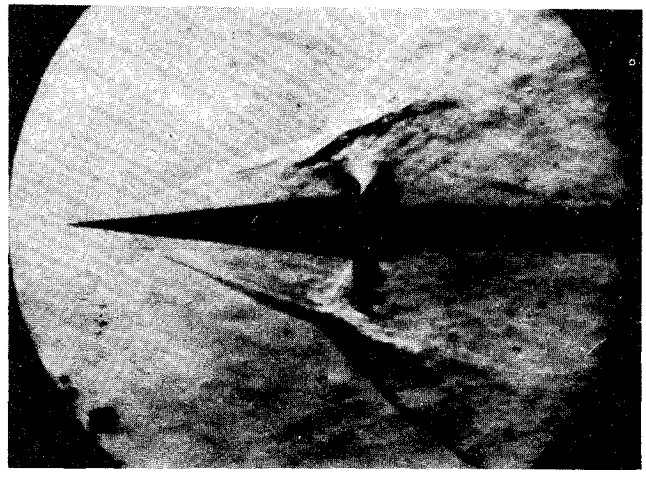

Fig. 2 Nitrogen injection, $\bar{m} = 3.13$, $M = 13.2$, $p_j^o = 35$ psia.

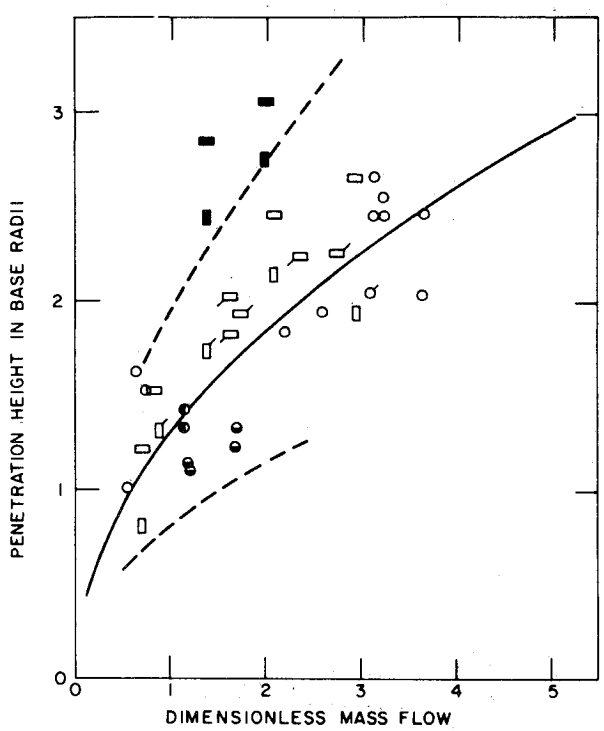

Fig. 3 Penetration height vs injectant mass flow.

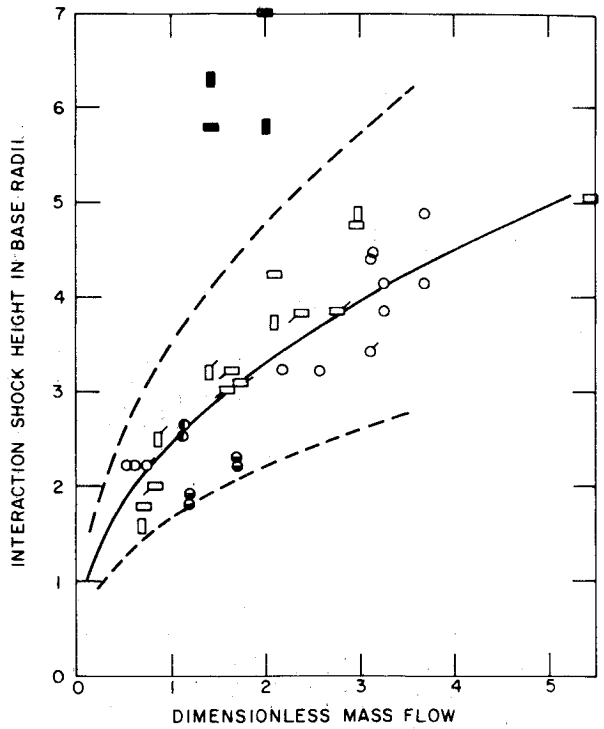

Fig. 4 Interaction shock height vs injectant mass flow.

We used the experimental measurements to determine which, if any, of these formulations properly model the effect of injectant gas properties on jet penetration into a hypersonic stream. The measured values of penetration height, normalized by the cone radius, are shown plotted vs dimensionless jet mass flow in Fig. 3. The symbols representing the test parameter variations are explained in Table 2: the symbol shape indicates the jet throat shape, the way the symbol is filled indicates the injectant gas, and the flags indicate pressure altitude. Before we compare the test results with the available formulations, four observations should be made. First, we believe a large part of the scatter in the data shown in the figures results from the unsteady nature of the interaction. Second, the data indicate no explicit effect upon penetration of the ambient pressure level at constant dimensionless mass flow, nor was such an effect expected. Third, the shape of the jet throat is unimportant, an observation consistent with our modeling of the jet as a point source and with the supersonic experiments of Schetz.[4] Fourth, a least squares regression through all the nitrogen data indicates the penetration height varies as the mass flow to a power between 0.4 and 0.5, thus generally verifying the point source model used in all the analyses.

Table 2 Symbol legend for Figs. 3 and 4

Jet throat shape, gas, altitude	Symbol
Circular orifice	○
10:1 slot orifice	▯
5:1 slot orifice	▬
N_2	○
He	●
Freon 116	◐
Xe	◒
151 kft	Unflagged
168 kft	○
195 kft	○
Theory[a,b] for N_2	———
Theory[a] for He	— — —
Theory[a] for Xe	- - - - - -

[a] In Fig. 3 the lines represent Eq. (3). In Fig. 4 the lines represent calculated shock height.
[b] This curve is also approximately correct for Freon 116.

In order to make a quantitative comparison of the data and the various formulations, we note that Eqs. (2) through (5) all have the form $h/r = k(\bar{m})^{1/2}$, where the coefficient k is a function primarily of the injectant gas properties. A comparison is given in Table 3 between the values of k computed from the four equations and the value of k determined experimentally, that is, the average experimental value of $h/r(\bar{m})^{1/2}$ for each injectant gas. Inspection of Table 3 indicates that the formulation of Zukoski and Spaid, Eq. (3), predicts the injection height very well, both qualitatively and quantitatively (within about 10%). The correlation of Schetz, Eq. (5), while generally yielding somewhat lower values, predicts the qualitative behavior of the penetration well except, not surprisingly, for the low gamma injectant. The blast

Table 3 Comparison of theory and experiment

Injectant gas	Molecular weight	Specific heat ratio	Coefficient k from: Eq. (2)	Eq. (3)	Eq. (4)	Eq. (5)[a]	Experiment
Nitrogen	28	1.40	2.08	1.26	1.12	0.84	1.39
Helium	4	1.67	2.53	1.89	1.79	1.27	2.10
Freon 116	138	1.085	2.02	1.17	0.77	0.62	1.25
Xenon	131	1.67	2.02	0.79	1.00	0.53	0.98

[a] Valid for injectant specific heat ratio of 1.4 only.

wave theory, Eq. (2), while predicting approximately the correct trends from gas to gas, predicts too little variation with injectant properties. Equation (4) works reasonably well for the gases with larger specific heat ratios, that is, the equation shows the proper dependence on molecular weight. However, Eq. (4) fails, even qualitatively, to predict the interaction enhancement derived from a low gamma injectant. In summary, the Zukoski and Spaid formulation is the best of the four in predicting the effect of the injectant gas on the penetration height and is also remarkably accurate. Equation (3) also means that the penetration height h is proportional to $(D_j{}^2 p_j{}^o)^{1/2}$, independent of $\mathcal{M}_j$, and a sufficiently weak function of γ_j that the greatest penetration that can be achieved for a given jet mass flow rate results from the use of the lightest injectant gas, regardless of its specific heat ratio. We have used Eq. (3) to correlate the data as shown by the three lines in Fig. 3.

The plenum or total temperature of the injectant gas was not varied during the test program and so the effect of the injectant temperature was not measured. Injectant total temperature, along with injectant molecular weight, affects the interaction by controlling the volume filled by the injectant as it expands to ambient pressure. This is reflected by the fact that $T_j{}^o$ appears only in the ratio $T_j{}^o/\mathcal{M}_j$ in each of the Eqs. (2–5). Since the Zukoski and Spaid model is physically accurate in the hypersonic regime, as our experiments indicate, and since the model successfully predicts the effect of the injectant molecular weight, we can reasonably expect the model to predict injectant temperature effects properly.

Having determined a method to predict the jet penetration height, it is a simple step to predict the interaction shock height. As suggested by the Zukoski and Spaid model, we replace the jet conceptually by a sphere of radius h calculated from Eq. (3), with its center at the jet orifice and then compute the resulting shock wave in the freestream flow. The shock tabulations of Chushkin and Shulishnina[5] are convenient for this task. The interaction shock heights in the plane of the cone base as computed and measured are shown in Fig. 4, where the symbols and lines have the meanings delineated in Table 2. The same general comments concerning scatter and the lack of effect of pressure altitude and nozzle geometry which were made with reference to the data in Fig. 3 apply to these data as well. The interaction shock height computation is accurate for the heavier gases but predicts a shock height for the helium injectant tests that is about 25% below the measured value.

References

[1] Broadwell, J., "Analysis of the Fluid Mechanics of Secondary Injection for Thrust Vector Control," *AIAA Journal*, Vol. 1, No. 5, May 1963, pp. 1067–1075.

[2] Zukoski, E. and Spaid, F., "Secondary Injection of Gases Into a Supersonic Flow," *AIAA Journal*, Vol. 2, No. 10, Oct. 1964, pp. 1689–1696.

[3] Cassel, L., Davis, J., and Engh, D., "Lateral Jet Control Effectiveness Prediction for Axisymmetric Missile Configurations," Rept. RD-TR-68-5, June, 1968. Research and Development Directorate, McDonnell Douglas Astronautics Company, Santa Monica, Calif.

[4] Schetz, J., "Interaction Shock Shape for Transverse Injection," *Journal of Spacecraft and Rockets*, Vol. 7, No. 2, Feb. 1970, pp. 143–151.

[5] Chushkin, P. and Shulishnina, N., "Tables of Supersonic Flow About Blunted Cones," translated by J. Springfield, RAD-TM-62-63, Sept., 1962. Avco Corporation, Wilmington, Mass.